

AD-A139413

TECHNICAL
LIBRARY

AD #139413

TECHNICAL REPORT ARLCB-TR-84001

STRESS DISTRIBUTION IN A CYLINDRICAL BAR SUBJECTED TO CYCLIC TORSIONAL LOADING

P. C. T. CHEN

H. C. WU

JANUARY 1984



**US ARMY ARMAMENT RESEARCH AND DEVELOPMENT CENTER
LARGE CALIBER WEAPON SYSTEMS LABORATORY
BENET WEAPONS LABORATORY
WATERVLIET N.Y. 12189**

APPROVED FOR PUBLIC RELEASE; DISTRIBUTION UNLIMITED

DISCLAIMER

The findings in this report are not to be construed as an official Department of the Army position unless so designated by other authorized documents.

The use of trade name(s) and/or manufacture(s) does not constitute an official indorsement or approval.

DISPOSITION

Destroy this report when it is no longer needed. Do not return it to the originator.

20. ABSTRACT (CONT'D)

condition is presented for all cycles until a steady loop is reached. The stress distributions in a cylindrical bar at different stages of loading and unloading are calculated. Some numerical results are presented.

TABLE OF CONTENTS

	<u>Page</u>
INTRODUCTION	1
ENDOCHRONIC THEORY	2
CYCLIC SHEAR RESPONSE	3
CYLINDRICAL BAR UNDER TORSION	5
NUMERICAL RESULTS AND DISCUSSION	7
REFERENCES	9

LIST OF ILLUSTRATIONS

1. Cyclic Shear Stress-Shear Strain Curve.	11
2. Torque vs. Outer Shear-Strain Curve.	12
3. Stress Distribution During Initial Loading.	13
4. Stress Distribution During First Unloading.	14
5. Stress Distribution During First Reloading.	15
6. Distribution of Residual Stresses in Second Cycle.	16

INTRODUCTION

In recent years much research has been devoted to developing realistic constitutive equations to describe complex material behavior such as cyclic plasticity (refs 1-9). The majority of these works are along the lines of the classical theory of plasticity. However, some attempts have also been made to establish new and independent theories. The endochronic theory developed by Valanis (ref 8) is based on the notion of intrinsic time and thermodynamic theory of internal variables. The original definition of intrinsic time has led to difficulties in cases where the history of deformation involved unloading. Valanis (ref 9) has since introduced a new concept of intrinsic time to overcome these difficulties. The new theory has been successfully applied to describe the cyclic hardening phenomenon under uniaxial loading (ref 10).

In this report the modified version of the endochronic theory of plasticity is applied to the problem of a cylindrical bar subjected to cyclic fully-reversed torsional loading. The governing equations of integral form are presented for pure shear deformation. Analytical techniques are employed in the solution of these equations. The stress distributions in a cylindrical bar at different stages of loading, unloading, and reloading are calculated. The solution for this problem based on a numerical iterative technique was reported recently (ref 11). A different approach and additional numerical results are presented here.

References are listed at the end of this report.

ENDOCHRONIC THEORY

According to the modified version of the endochronic theory of plasticity (ref 9), the intrinsic time ζ for the one-dimensional case is defined by

$$d\zeta = \left| d\gamma - k_1 \frac{d\tau}{\mu_0} \right| \quad (1)$$

where k_1 is a positive scalar such that $0 \leq k_1 \leq 1$, τ and γ are shear stress and strain respectively, and μ_0 is the shear modulus. When $k_1 = 0$, the original form of intrinsic time is recovered; but when $k_1 = 1$, $\Omega = \gamma - (\tau/\mu_0)$ is the plastic strain, and

$$d\zeta = |d\Omega| \quad (2)$$

Equation (2) is used throughout this investigation so that the concept of plastic strain may be incorporated into the present development.

In the case of pure shear, the governing constitutive equation of integral form is given by

$$\tau = \mu_0 \int_0^z \rho(z-z') \frac{d\Omega}{dz'} dz' \quad (3)$$

where

$$\mu_0 \rho(z) = \mu_0 \rho_0 \delta(z) + \mu_1 e^{-\alpha z} + \mu_2 \quad (4)$$

in which ρ_0 , α , μ_1 , and μ_2 are material parameters; $\delta(z)$ is the delta function.

A more general form of the intrinsic time measure involving the strain rate effect is proposed in Reference 10 as

$$d\zeta = k(|\dot{\Omega}|) |d\Omega| \quad (5)$$

where k , the strain rate sensitivity function, is a function of $\dot{\Omega}$. In this case, Eq. (3) can be written as

$$\tau = \mu_0 \int_0^z \rho(z-z') \left[\pm \frac{1}{k} \right] \frac{d\zeta}{dz'} dz' \quad (6)$$

The constitutive Eq. (6) is applied here to describe the material behavior at constant plastic strain rate. The intrinsic time z is related to ζ by the following time scale

$$\frac{d\zeta}{dz} = f(\zeta) \quad (7)$$

where $f(\zeta)$ describes isotropic hardening and is, therefore, termed the hardening function. In this report, the form

$$f(z) = c - (c-1)e^{-\beta z} \quad (8)$$

is used because of its simplicity and its proved usefulness in cases of cyclic loading (ref 10). The parameters c and β are material constants.

CYCLIC SHEAR RESPONSE

By using the hardening function given in Eq. (8), the constitutive equation for loading with constant plastic strain rate is written as

$$\tau = (\mu_0/k) \int_0^z \rho(z-z') f(z') dz' \quad (9)$$

where $\rho(z)$ is defined by Eq. (4) and k is a constant. Integrating Eq. (9), the following explicit result is obtained:

$$\tau = (\tau_y/k) f(z) + (\mu_1/k)(g(z)-g(0)) + (\mu_2/k)h(z) \quad (10)$$

where

$$\tau_y = \mu_0 \rho_0 \text{ is the yield stress} \quad (11)$$

$$h(z) = cz + \beta^{-1}(c-1)(e^{-\beta z}-1) \quad (12)$$

$g(z)$, $g(0)$ are the values of the function $g(z')$ evaluated at $z' = z$, 0 , respectively, and

$$g(z') = (c/\alpha)e^{-\alpha(z-z')} - (c-1)/(\alpha-\beta)e^{-\alpha z + (\alpha-\beta)z'} \quad (13)$$

Equation (10) is now the response function for loading. If unloading occurs when the plastic strain reaches Ω_1 (or $z = z_1$), then the response function for $z > z_1$ can be obtained as

$$\tau = -(\tau_y/k)f(z) + (\mu_1/k)[-g(z) + 2g(z_1) - g(0)] + (\mu_2/k)[-h(z) + 2h(z_1)] \quad (14)$$

If Eqs. (10) and (14) are examined at $z = z_1^-$ and z_1^+ , respectively, a drop in stress of $2(\tau_y/k)f(z_1)$ results during elastic unloading.

If reloading takes place after unloading and, assuming that reloading occurs at $\Omega = \Omega_2$ (or $z = z_2$, where $z_2 > z_1$), the response function for $z > z_2$ is obtained as

$$\begin{aligned} \tau = & (\tau_y/k)f(z) + (\mu_1/k)[g(z) - 2g(z_2) + 2g(z_1) - g(0)] \\ & + (\mu_2/k)[h(z) - 2h(z_2) + 2h(z_1)] \end{aligned} \quad (15)$$

When Eqs. (14) and (15) are examined at $z = z_2^-$ and z_2^+ , respectively, a jump in stress of $2(\tau_y/k)f(z_2)$ is again obtained during elastic reloading.

This procedure of obtaining a theoretical expression for each part of the cyclic loading process may be continued. Thus, a general expression of the response function for the constant total strain amplitude cyclic torsion test may be found to be

$$\tau = (-1)^N(\tau_y/k)f(z) + (\mu_1/k)G(z) + (\mu_2/k)\Omega(z) \quad (16)$$

where

$$G(z) = (-1)^N[g(z) - g(z_N)] + \sum_{n=1}^N (-1)^{n+1}[g(z_n) - g(z_{n-1})] \quad (17)$$

$$\Omega(z) = (-1)^N[h(z) - h(z_N)] + \sum_{n=1}^N (-1)^{n+1}[h(z_n) - h(z_{n-1})] \quad (18)$$

Note that $N \neq 0$ is the number of half-cycles, odd for unloading and even for reloading.

After many cycles when the values of z become large, the hysteresis loop of the stress-strain curve will approach a steady state. If Eq. (16) is examined at $z = z_N^-$ and $z = z_N^+$, a drop or jump in stress of magnitude $2(\tau_y/k)f(z_N)$ results, which corresponds to the elastic response upon the reversal of the loading or unloading direction. When z_N is sufficiently large, the jump or drop of stress becomes a constant value $2c \tau_y/k$ at the steady state.

CYLINDRICAL BAR UNDER TORSION

For a cylindrical bar under torsional loading, the external torque is

$$T_s = 2\pi \int_0^{r_a} \tau r^2 dr \quad (19)$$

where τ is the current shear stress corresponding to location r , and r_a is the radius of cross-section. Geometric considerations show that radial lines have to remain straight after deformation. Thus, one concludes that

$$\gamma = (\gamma_a/r_a)r \quad (20)$$

where γ_a is the strain at the outermost fiber. Since a yield stress is introduced in Eq. (4), an elastic core always exists during deformation whose radius r_e is given by

$$r_e = \frac{\tau_y}{\mu_0} \frac{r_a}{\gamma_a} \quad (21)$$

If the experiment is strain-controlled with strain at r_a varying between $-\gamma_a$ and $+\gamma_a$, and with γ_a in the plastic range, then the torque can be computed as

$$T_s = \frac{\pi}{2} \tau_y r_e^3 + 2\pi(r_a/\gamma_a)^3 \int_{\gamma_e}^{\gamma_a} \tau \gamma^2 d\gamma \quad (22)$$

where

$$\gamma_e = (\gamma_a/r_a)r_e, \quad \gamma = \Omega + \tau/\mu_0 \quad (23)$$

τ and Ω are given by Eqs. (16) and (18), respectively.

Now that γ is known, the values of z and τ at each fiber can be calculated and used in Eq. (22). Note that there exists an explicit expression for all cycles

$$d\gamma/dz = \Omega'(z) + \frac{1}{\mu_0} \tau'(z) = p(z) \quad (24)$$

where

$$\begin{aligned} \Omega'(z) &= (-1)^N f'(z), \quad f'(z) = \beta(c-1)e^{-\beta z} \\ \tau'(z) &= (-1)^N [\tau_y/k] f'(z) + (\mu_2/k) f(z) + (\mu_1/k) \Gamma'(z) \\ \Gamma'(z) &= (-1)^N [F'_{zz} - F'_{Nz}] - \sum_{n=1}^N (-1)^n [F'_{nz} - F'_{(n-1)z}] \\ F'_{zz} &= [\beta(c-1)/(\alpha-\beta)] e^{-\beta z}, \quad F'_{nz} = -\alpha F_{nz} \end{aligned}$$

and

$$F_{nz} = \frac{c}{\alpha} e^{-\alpha(z-z_n)} - \left(\frac{c-1}{\alpha-\beta}\right) e^{-\alpha z} + (\alpha-\beta) z_n \quad (25)$$

The integral in Eq. (22) can be replaced by

$$\int_{\gamma_e}^{\gamma_a} \tau \gamma^2 d\gamma = \int_0^{z_a} \tau \gamma^2 p(z) dz \quad (26)$$

where z_a can be calculated by Eq. (23) with known value γ_a . Now the numerical integration becomes very easy because the values of the integrand can be evaluated directly.

NUMERICAL RESULTS AND DISCUSSION

To apply the developed model, the material constants (α , β , c , τ_y , μ_0 , μ_1 , μ_2) in the theory have to be determined. These material constants can be determined if the cyclic shear stress-strain curve for the material has been obtained experimentally. The usual procedure is to perform a cyclic torsion test using a thin-walled tubular specimen. Such a test for the annealed AISI 4142 steel was carried out by the Plasticity Research Laboratory at the University of Iowa. The values of constants were then used to predict the results for a solid bar test. The theoretical and experimental results were in reasonable agreement (ref 11). This real material did not show any appreciable amount of cyclic hardening.

For purpose of investigating the implications of the developed model, a hypothetical material with appreciable cyclic hardening behavior was studied. The shear stress-strain behavior of such material under fully-reversed torsional loading is presented in Figure 1. The material constants were determined as: $\alpha = 1000$, $\beta = 50$, $c = 1.5$, $\tau_y = 10^4$ psi, $\mu_0 = 10^7$ psi, $\mu_1 = 4 \times 10^6$ psi, $\mu_2 = 0$. A steady loop was established after a few cycles. The same set of constants was then used to predict the stress distribution in a cylindrical bar subjected to cyclic torsional loading. We carried out the computational process seven cycles after initial loading. The numerical results are presented here for the initial loading half-cycle and two cycles of unloading and reloading.

Figure 2 presents the numerical results for the torque as related to the shear strain at the outermost fiber. The distribution of stress in the cross-section at different magnitudes of torque during the initial loading

half-cycle is presented in Figure 3. The corresponding shear strains at the outer fiber are 0.1, 0.3, 0.6, and 1.0 percent, respectively. Notice that the outer fiber is the first one to yield at $\gamma_a = 0.1$ percent; subsequently as more torque is applied, the radius of the elastic inner core gets smaller. Also notice that the rate of hardening for each fiber decreases which is, of course, in accordance with strain hardening phenomena.

Figure 4 presents the distribution of the shear stress in the bar at three stages of the first unloading half-cycle. The top and bottom curves correspond to the beginning and end of the unloading stages, i.e., $\gamma_a = \pm 1$ percent. The corresponding values of torque are 1256, -1387 lb-in., respectively. The middle curve represents the residual stress distribution when the applied torque is equal to zero. A few iterations are needed to reach this state and the residual shear strain at the outermost fiber is 0.378 percent. Figure 5 presents the distribution of the shear stress in the bar at three stages of the first reloading half-cycle, i.e., $T_s = -1387, 0, 1461$ lb-in. The middle curve represents the distribution of residual stress when the torque is equal to zero. Reverse yielding occurs within the outer 12 percent of the section when $T_s = 0$ during unloading and reloading. The distribution of residual stress during unloading is quite different from that during reloading as shown in Figures 4 and 5 for the first cycle. Similar results for the residual stress distribution during the second unloading-reloading cycle are shown in Figure 6. The solid curve is the favorable one if the applied torque during service is in the same direction as the initial loading.

REFERENCES

1. Z. Mroz, "Simplified Theories of Cyclic Plasticity," ACTA MECHANICA, Vol. 22, pp. 131-152, 1975.
2. A. Miller, "An Inelastic Constitutive Model for Monotonic, Cyclic, and Creep Deformation: Part I - Equations, Development, and Analytical Problems," J. Eng. Materials and Tech., Vol. 98, pp. 97-105, 1976.
3. M. A. Eisenberg, "A Generalization of Plastic Flow Theory With Application to Cyclic Hardening and Softening Phenomena," J. Eng. Materials and Tech., Vol. 98, pp. 221-228, 1976.
4. E. Krempl, M. C. M. Liu, and D. C. Nairn, "An Exponential Stress-Strain Law for Cyclic Plasticity," J. Eng. Materials and Tech., Vol. 98, pp. 322-329, 1976.
5. E. P. Popov and H. Peterson, "Cyclic Metal Plasticity: Experiment and Theory," J. Eng. Mech. Div., Proc. ASCE, Vol. 104, EM6, pp. 1371-1388, 1978.
6. S. R. Bodner and I. Partom, "Uniaxial Cyclic Loading of Elasto-Viscoplastic Materials," J. Appl. Mech., Vol. 46, pp. 805-810, 1979.
7. D. C. Drucker and L. Palgen, "On Stress-Strain Relations Suitable for Cyclic and Other Loading," J. Appl. Mech., Vol. 48, pp. 479-485, 1981.
8. K. C. Valanis, "A Theory of Viscoplasticity Without a Yield Surface, Part I and Part II," Archives of Mechanics, Vol. 23, pp. 517-551, 1971.
9. K. C. Valanis, "Fundamental Consequences of a New Intrinsic Time Measure-Plasticity as a Limit of the Endochronic Theory," Archives of Mechanics, Vol. 32, pp. 171-191, 1980.

10. H. C. Wu and M. C. Yip, "Endochronic Description of Cyclic Hardening Behavior for Metallic Materials," J. of Eng. Materials and Technology, Vol. 103, pp. 212-217, 1981.
11. P. C. T. Chen, M. R. Aboutorabi, and H. C. Wu, "Cyclic Torsion of a Circular Cylinder," Proc. of 8th Army Symposium on Solid Mechanics, AMMRC MS82-4, pp. 405-415, 1982.

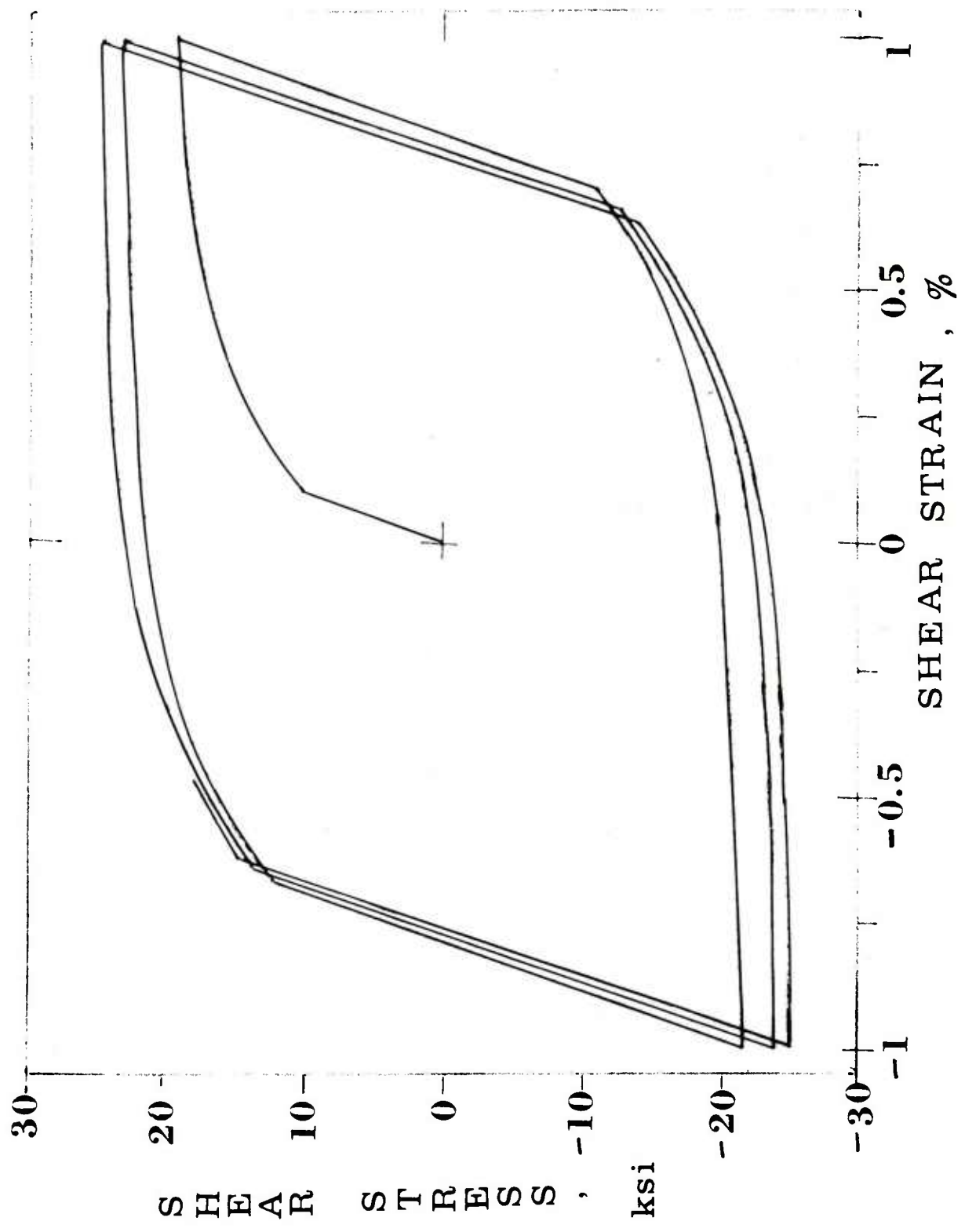


Figure 1. Cyclic Shear Stress-Shear Strain Curve.

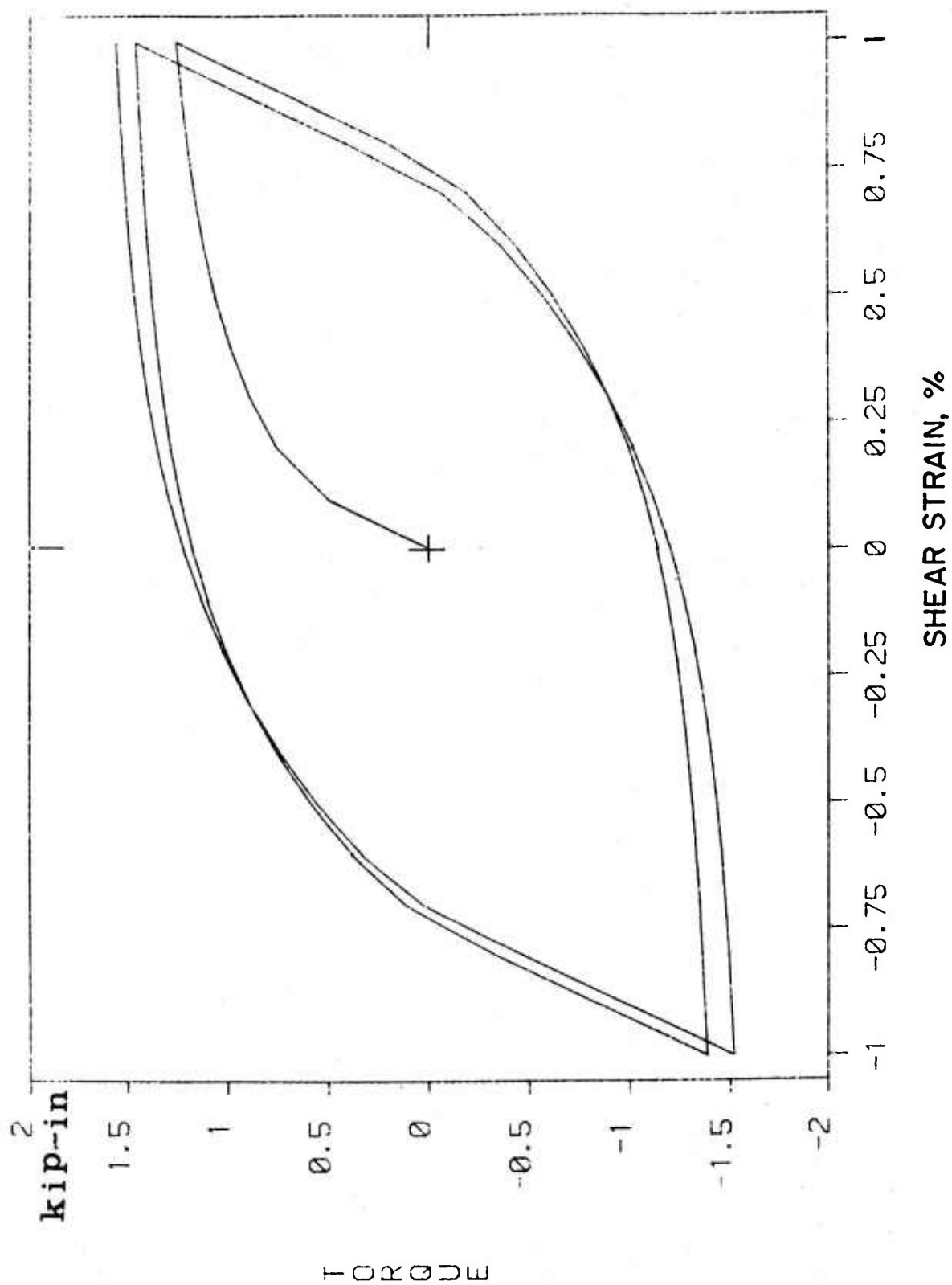


Figure 2, Torque vs. Outer Shear-Strain Curve.

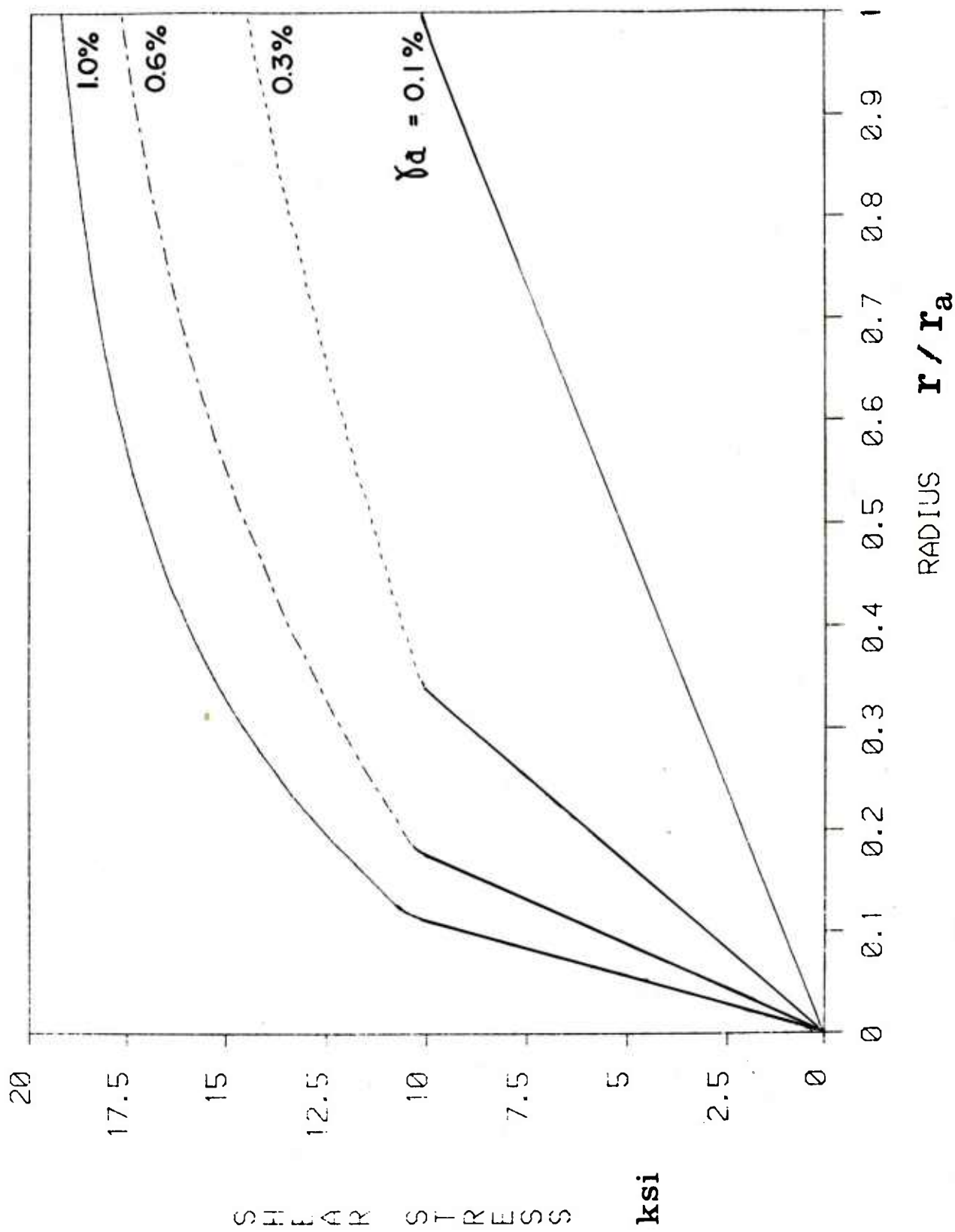


Figure 3. Stress Distribution During Initial Loading.

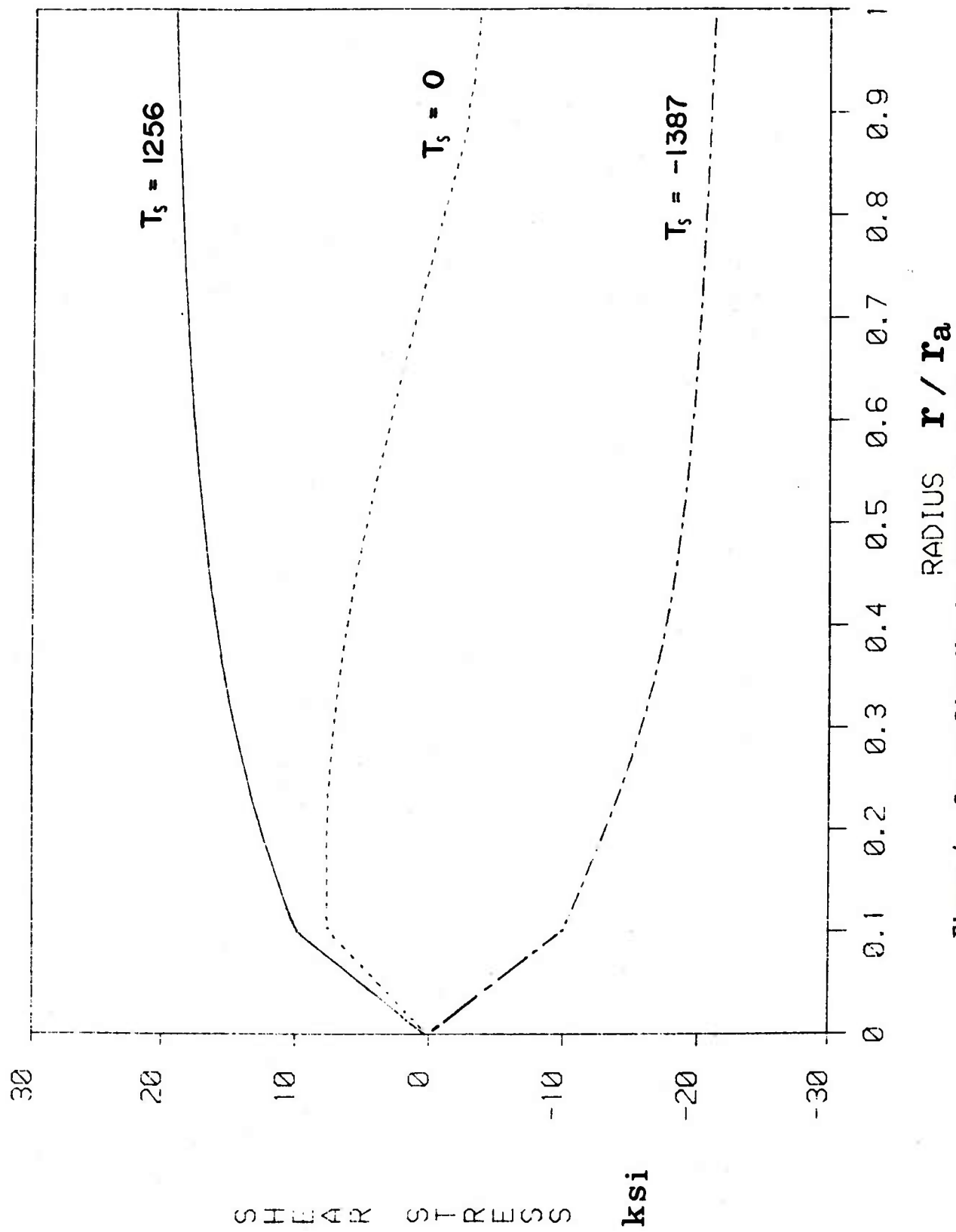


Figure 4. Stress Distribution During First Unloading.

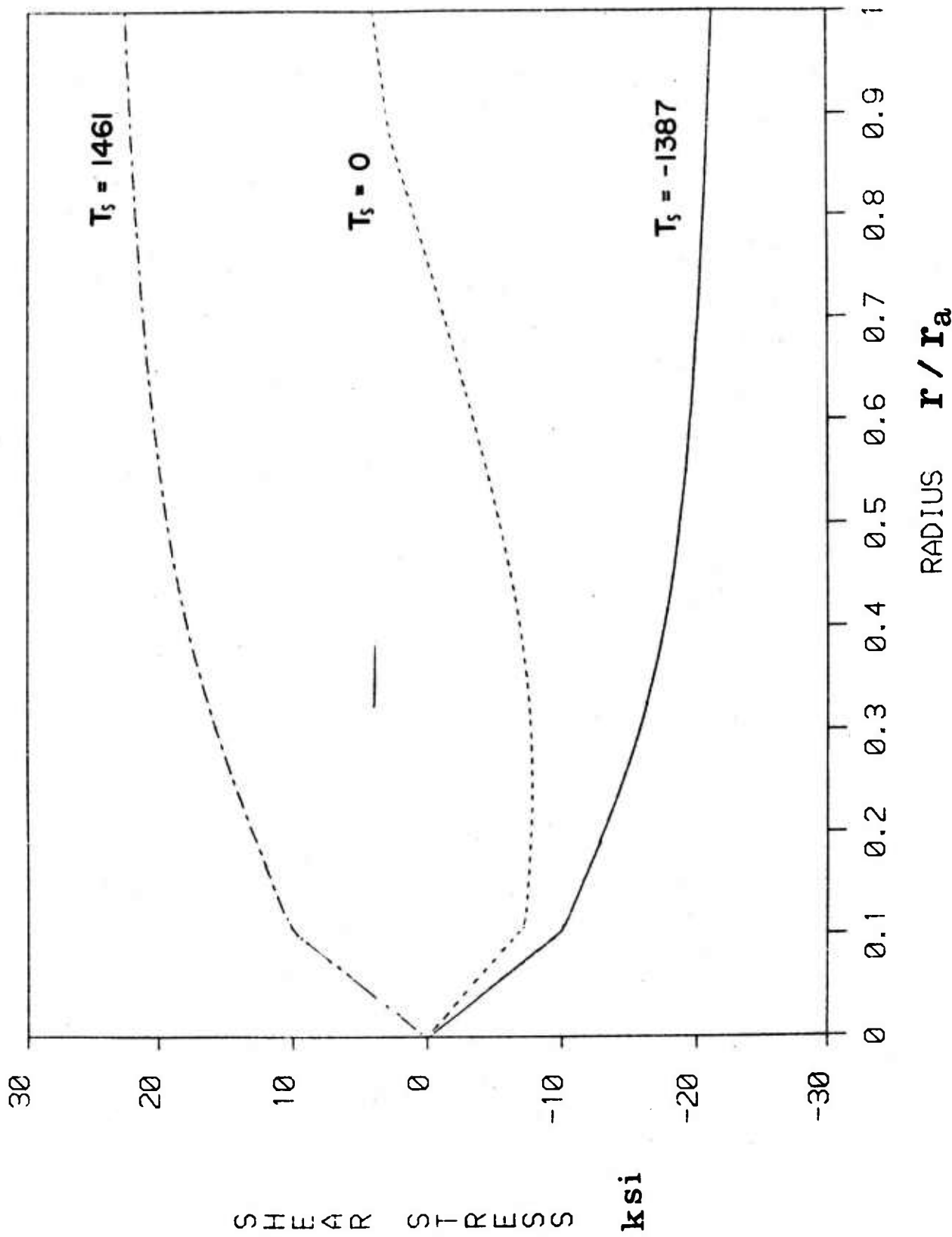


Figure 5. Stress Distribution During First Reloading.

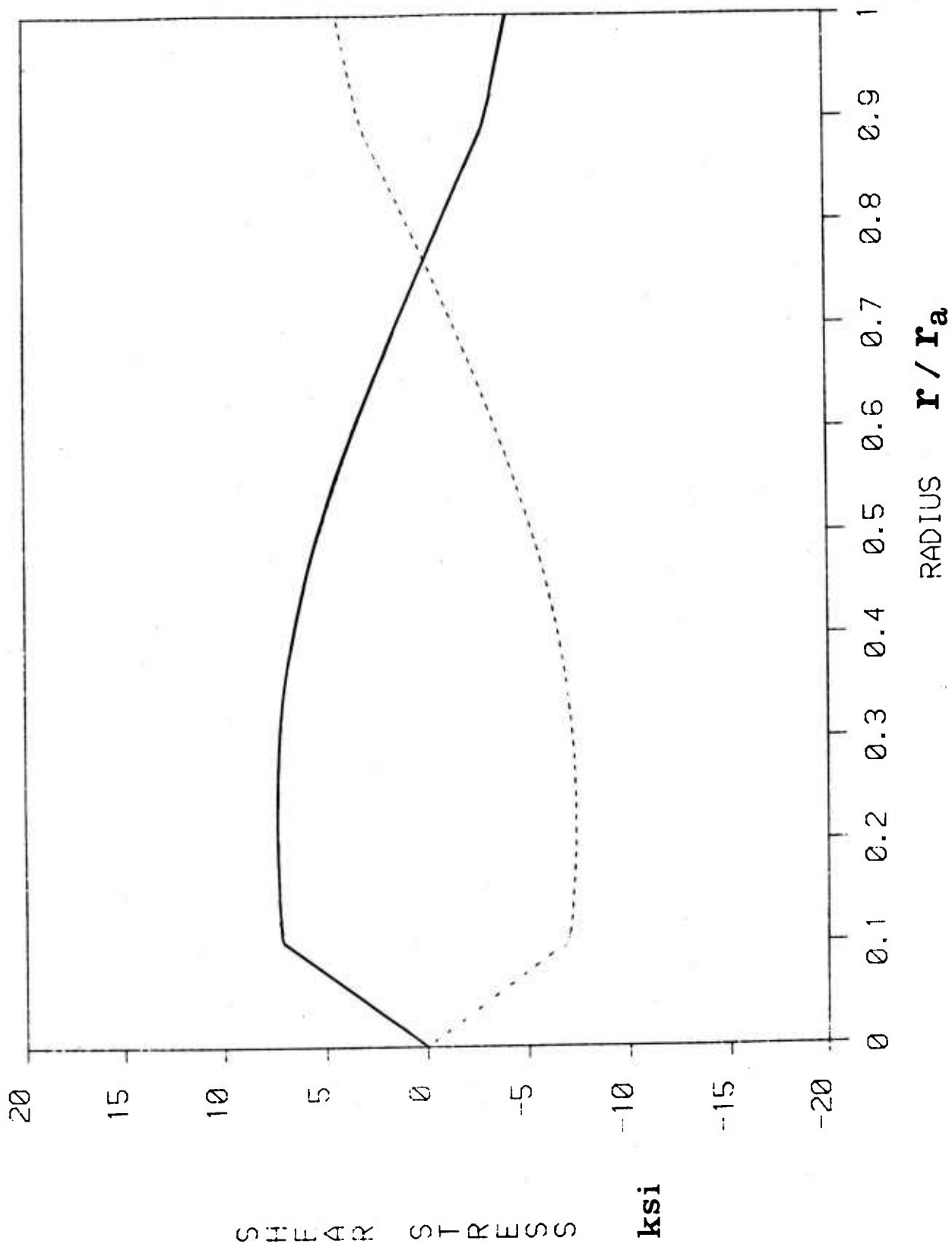


Figure 6. Distribution of Residual Stresses in Second Cycle.

TECHNICAL REPORT INTERNAL DISTRIBUTION LIST

	<u>NO. OF COPIES</u>
CHIEF, DEVELOPMENT ENGINEERING BRANCH	
ATTN: DRSMC-LCB-D	1
-DP	1
-DR	1
-DS (SYSTEMS)	1
-DS (ICAS GROUP)	1
-DC	1
CHIEF, ENGINEERING SUPPORT BRANCH	
ATTN: DRSMC-LCB-S	1
-SE	1
CHIEF, RESEARCH BRANCH	
ATTN: DRSMC-LCB-R	2
-R (ELLEN FOGARTY)	1
-RA	1
-RM	1
-RP	1
-RT	1
TECHNICAL LIBRARY	5
ATTN: DRSMC-LCB-TL	
TECHNICAL PUBLICATIONS & EDITING UNIT	2
ATTN: DRSMC-LCB-TL	
DIRECTOR, OPERATIONS DIRECTORATE	1
DIRECTOR, PROCUREMENT DIRECTORATE	1
DIRECTOR, PRODUCT ASSURANCE DIRECTORATE	1

NOTE: PLEASE NOTIFY DIRECTOR, BENET WEAPONS LABORATORY, ATTN: DRSMC-LCB-TL,
OF ANY ADDRESS CHANGES.

TECHNICAL REPORT EXTERNAL DISTRIBUTION LIST

	<u>NO. OF COPIES</u>		<u>NO. OF COPIES</u>
ASST SEC OF THE ARMY RESEARCH & DEVELOPMENT ATTN: DEP FOR SCI & TECH THE PENTAGON WASHINGTON, D.C. 20315	1	COMMANDER US ARMY AMCCOM ATTN: DRSMC-LEP-L(R) ROCK ISLAND, IL 61299	1
COMMANDER DEFENSE TECHNICAL INFO CENTER ATTN: DTIC-DDA CAMERON STATION ALEXANDRIA, VA 22314	12	COMMANDER ROCK ISLAND ARSENAL ATTN: SMCRI-ENM (MAT SCI DIV) ROCK ISLAND, IL 61299	1
COMMANDER US ARMY MAT DEV & READ COMD ATTN: DRCDE-SG 5001 EISENHOWER AVE ALEXANDRIA, VA 22333	1	DIRECTOR US ARMY INDUSTRIAL BASE ENG ACTV ATTN: DRXIB-M ROCK ISLAND, IL 61299	1
COMMANDER ARMAMENT RES & DEV CTR US ARMY AMCCOM ATTN: DRSMC-LC(D) DRSMC-LCE(D) DRSMC-LCM(D) (BLDG 321) DRSMC-LCS(D) DRSMC-LCU(D) DRSMC-LCW(D) DRSMC-SCM-O (PLASTICS TECH EVAL CTR, BLDG. 351N) DRSMC-TSS(D) (STINFO) DOVER, NJ 07801	1 1 1 1 1 1 1 2	COMMANDER US ARMY TANK-AUTMV R&D COMD ATTN: TECH LIB - DRSTA-TSL WARREN, MI 48090 COMMANDER US ARMY TANK-AUTMV COMD ATTN: DRSTA-RC WARREN, MI 48090 COMMANDER US MILITARY ACADEMY ATTN: CHMN, MECH ENGR DEPT WEST POINT, NY 10996 US ARMY MISSILE COMD REDSTONE SCIENTIFIC INFO CTR ATTN: DOCUMENTS SECT, BLDG. 4484 REDSTONE ARSENAL, AL 35898	1 1 2
DIRECTOR BALLISTICS RESEARCH LABORATORY ARMAMENT RESEARCH & DEV CTR US ARMY AMCCOM ATTN: DRSMC-TSB-S (STINFO) ABERDEEN PROVING GROUND, MD 21005	1	COMMANDER US ARMY FGN SCIENCE & TECH CTR ATTN: DRXST-SD 220 7TH STREET, N.E. CHARLOTTESVILLE, VA 22901	1
MATERIEL SYSTEMS ANALYSIS ACTV ATTN: DRXY-MP ABERDEEN PROVING GROUND, MD 21005	1		

NOTE: PLEASE NOTIFY COMMANDER, ARMAMENT RESEARCH AND DEVELOPMENT CENTER,
US ARMY AMCCOM, ATTN: BENET WEAPONS LABORATORY, DRSMC-LCB-TL,
WATERVLIET, NY 12189, OF ANY ADDRESS CHANGES.

TECHNICAL REPORT EXTERNAL DISTRIBUTION LIST (CONT'D)

	<u>NO. OF COPIES</u>		<u>NO. OF COPIES</u>
COMMANDER US ARMY MATERIALS & MECHANICS RESEARCH CENTER ATTN: TECH LIB - DRXMR-PL WATERTOWN, MA 01272	2	DIRECTOR US NAVAL RESEARCH LAB ATTN: DIR, MECH DIV CODE 26-27, (DOC LIB) WASHINGTON, D.C. 20375	1 1
COMMANDER US ARMY RESEARCH OFFICE ATTN: CHIEF, IPO P.O. BOX 12211 RESEARCH TRIANGLE PARK, NC 27709	1	COMMANDER AIR FORCE ARMAMENT LABORATORY ATTN: AFATL/DLJ AFATL/DLJG EGLIN AFB, FL 32542	1 1
COMMANDER US ARMY HARRY DIAMOND LAB ATTN: TECH LIB 2800 POWDER MILL ROAD ADELPHIA, MD 20783	1	METALS & CERAMICS INFO CTR BATTELLE COLUMBUS LAB 505 KING AVENUE COLUMBUS, OH 43201	1
COMMANDER NAVAL SURFACE WEAPONS CTR ATTN: TECHNICAL LIBRARY CODE X212 DAHLGREN, VA 22448	1		

NOTE: PLEASE NOTIFY COMMANDER, ARMAMENT RESEARCH AND DEVELOPMENT CENTER,
US ARMY AMCCOM, ATTN: BENET WEAPONS LABORATORY, DRSMC-LCB-TL,
WATERVLIET, NY 12189, OF ANY ADDRESS CHANGES.

READER EVALUATION

Please take a few minutes to complete the questionnaire below and return to us at the following address: Commander, Armament Research and Development Center, U.S. Army AMCCOM, ATTN: Technical Publications, DRSMC-LCB-TL, Watervliet, NY 12189.

1. Benet Weapons Lab. Report Number _____

2. Please evaluate this publication (check off one or more as applicable).

	Yes	No
Information Relevant	_____	_____
Information Technically Satisfactory	_____	_____
Format Easy to Use	_____	_____
Overall, Useful to My Work	_____	_____
Other Comments	_____	

3. Has the report helped you in your own areas of interest? (i.e. preventing duplication of effort in the same or related fields, savings of time, or money). _____

4. How is the report being used? (Source of ideas for new or improved designs. Latest information on current state of the art, etc.). _____

5. How do you think this type of report could be changed or revised to improve readability, usability? _____

6. Would you like to communicate directly with the author of the report regarding subject matter or topics not covered in the report? If so please fill in the following information.

Name: _____

Telephone Number: _____

Organization Address: _____